Electronic Supplementary Material (ESI) for Energy & Environmental Science.

Supplementary Information

High-performance magnesium metal battery via switching passivation film into solid electrolyte interphase

Jiwoong Bae,‡ Hyoju Park,‡ Xuelin Guo, Xiao Zhang, Jamie H. Warner, Guihua Yu*

‡Contributed equally to this work

*Correspondence to: ghyu@austin.utexas.edu

METHODS AND CHARACTERIZATION

Preparation of Zn-skeleton

For the interphase investigation, Mg-metal ribbons were used, with a thickness of 250 μm, a width of 5 mm, and a length of 10 mm. Before coating Zn-skeleton, one side of Mg-metal ribbons was carefully scratched with blades in the glove box to remove the native oxide layer. For the electrochemical test, Mg powder was used instead of the Mg ribbon. To prepare the slurry, Mg powder, super P and PVDF binder were mixed in N-Methyl-2-Pyrrolidone (NMP) solvent with a ratio of 8:1:1. The slurry was coated on stainless-steel foils and dried at 80 ^{o}C for 2 hrs. The mass loading was about 10 mg cm^{-2}. For the Zn-skeleton preparation, the surface scratched Mg-metal ribbon, or the Mg powder electrode was immersed in 5 mL of 1 M $ZnCl_2$ in the THF solution. After 30 min, the Zn-skeleton was coated on Mg-metal (Zn-skeleton), which was rinsed by THF and PC, respectively. All the procedures were conducted in the glove box.

Interphase Film Characterization

SEM-EDX investigated the morphology and elemental distribution with a Hitachi S-5500 SEM. STEM imaging, STEM-EDX, and STEM-EELS were conducted using an aberration-corrected JEOL NEOARM operated at 80 kV. After the electrochemical test, all the samples were rinsed by THF and PC, respectively and dried in the glove box. For the sample preparation of STEM, the sample surface was carefully scratched into the ethanol solvent, and the solution was dropped on the TEM grid to obtain the interphase debris. XRD patterns were investigated by a Rigaku MiniFlex 600 X-ray diffraction system. The XRD samples were covered and sealed by Kapton film to protect the samples from unnecessary air oxidation. For the interphase compositional analysis, XPS was performed using Kratos Axis Ultra DLD X-ray Photoelectron Spectrometer equipped with a monochromatic Al Kα X-ray source (1,486.7 eV) for excitation.

Symmetric and Asymmetric Cell Test

For the symmetric cell test, Mg powder electrodes were assembled in a coin cell with glass fiber as a separator in which 100 μL of 0.5 M $Mg(ClO_4)_2$ in PC was injected as an electrolyte. The Zn-skeleton electrodes were prepared with immersing Mg powder electrodes in 1M $ZnCl_2$ in THF solution, which was electrochemically magnesiated for 30 min at 0.01 mA/cm^2 in the same electrolyte before assembling into the coin cell. The current density of 0.01 mA/cm^2 was applied for 30 min plating and 30 min stripping.

For the long-term plating test, the Mg powder electrode was used as a reference and counter electrode, while either bare Mg ribbon or Zn-skeleton ribbon was used as working electrode. 100 μL of 0.5 M $Mg(ClO_4)_2$ in PC was used as an electrolyte in glass fiber. The current density of 0.01 mA/cm^2 was applied continuously until the voltage reaches the cut-off voltage of – 5.0V.

For the asymmetric cell test, an Mg ribbon was used as a reference and counter electrode, while Zn foil or Zn-skeleton coated Mg ribbon was used as a working electrode. The cell was assembled in a coin cell with glass fiber as a separator in which 100 μL of 0.5 M PhMgCl in THF was injected as an electrolyte. The bare metal foils, such as Mg ribbon or Zn foil, were scratched by blades to remove the native oxide layer before assembly.

EIS was conducted to measure symmetric cells' impedance with the frequency range from 1 MHz to 30 mHz with coin cells. The temperature was changed to measure the activation energy in the Arrhenius plot from 30 to 60 ˚C.

Mg-Li Hybrid Battery Test

For the cathode preparation, the active materials (i.e., NCM powders) were mixed with super P and PVDF binder in NMP solvent with a ratio of 8:1:1. The slurry was then coated on Al foil for NCM cathode, dried in 80 ^oC oven for 2 hrs. The Mg-Li hybrid batteries were assembled in a coin cell where a glass fiber was

used as a separator. 50 μL of 0.5 M $MgTFSI_2$ + 3 M LiTFSI in PC was used as an electrolyte. The outer cathode area on the stainless-steel cathode cap was covered with Kapton tape to minimize the electrolyte's corrosion with the cell component. The cut-off voltages for the NCM battery were 1.0 – 3.5 V for 0.1 C and 1.5 – 3.5 V for 0.5 C. The Li | NCM batteries were assembled with the same components as the Zn-skeleton | NCM battery except that Li-metal foil was used instead of Zn-skeleton. The cut-off voltage was 2.7 – 4.25 V.

Theoretical Calculation of Energy Density

The theoretical energy density (Wh kg^{-1}) of Li-ion, Mg-Li hybrid, and Mg-ion batteries were calculated by the energy of a cell (mWh cm^{-2}) divided by the total weight (g cm^{-2}).

1. The energy of a cell (mWh cm^{-2})

The energy of a cell was calculated based on the cell capacity multiplied by discharge-mid-voltage. The same specific capacity (150 mAh g^{-1}) of active materials (20 mg cm^{-2}) was used for all three types of cells, while different working voltages of 3.7 V (Li-ion), 2.82 V (Mg-Li hybrid) and 3 V (Mg-ion) were assumed. Therefore, the energy was calculated by specific capacity (150 mAh g^{-1}) * mass loading (20 mg cm^{-2}) * discharge-mid-voltage (V). As a result, each cell would have 11.1 mWh cm^{-2} (Li-ion), 8.46 mWh cm^{-2} (Mg-Li hybrid) and 9 mWh cm^{-2} (Mg-ion).

2. The weight of each cell component

The densities of materials for current collectors are Cu (8.96 g cm^{-3}), Al (2.7 g cm^{-3}), Mg (1.74 g cm^{-3}), and Zn (7.14 g cm^{-3}). The thickness for each component is assumed to be 8 μm (Cu), 12 μm (Al), 8 μm (Mg), and 5 μm (Zn). By multiplying the thickness and the density, we could achieve the weight of the current collector per area; 10.84 mg cm^{-2} (Li-ion) and 4.96 mg cm^{-2} (Mg-Li hybrid & Mg-ion).

The electrolyte for Li-ion and Mg-ion batteries are assumed to be 2.4 mg cm^{-2} based on the electrolyte density. However, the electrolyte weight of the Mg-Li hybrid battery is proportional to the cathode weight, which has been calculated by the number of Mg ions required. For 3 mAh cm^{-2}, 263 mg of 0.5 M $MgTFSI_2$ + 3 M LiTFSI in PC electrolyte is required.

As we mentioned above, the cathode weight was fixed to be 20 mg cm^{-2}, and we assumed 1/2 of cathode weight to be the anode weight for the Li-ion battery (10 mg cm^{-2}). We assumed 0 mg cm^{-2} for the anode of Mg-Li hybrid and Mg-ion batteries since the Zn-skeleton's weight had been included in the current collector.

3. Energy density

To sum up, the energy density was calculated based on the energy (mWh cm^{-2}) of a cell divided by the total weight of the cell components (mg cm^{-2}).

- Li-ion battery: 11.1 mWh cm^{-2} / 42.8 mg cm^{-2} = 259 Wh kg^{-1}
- Mg-Li hybrid battery: 8.46 mWh cm^{-2} / 291.8 mg cm^{-2} = 29 Wh kg^{-1}
- Mg-ion battery: 9 mWh cm^{-2} / 30.6 mg cm^{-2} = 294 Wh kg^{-1}

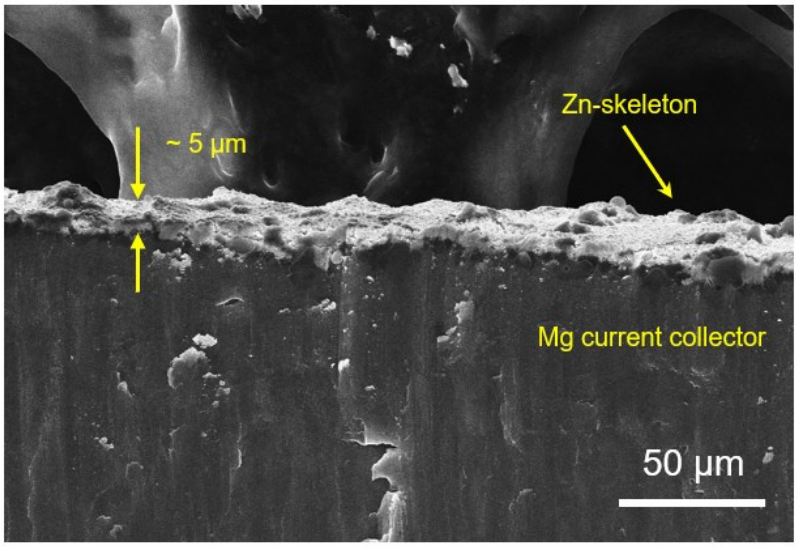

Figure S1. Cross-sectional SEM image of an as-prepared Zn-skeleton.

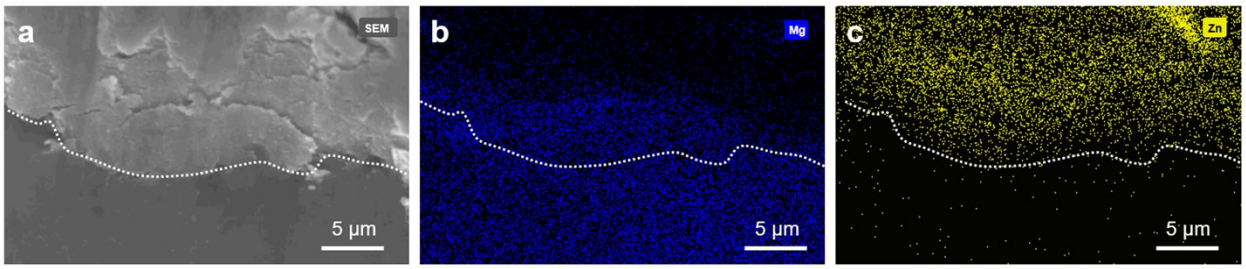

Figure S2. a) The SEM and elemental mapping of b) Mg and c) Zn at the interface between Zn-skeleton and Mg current collector. Overlapping of Mg and Zn at the interface may indicate the strong adhesion of Zn-skeleton on the Mg current collector.

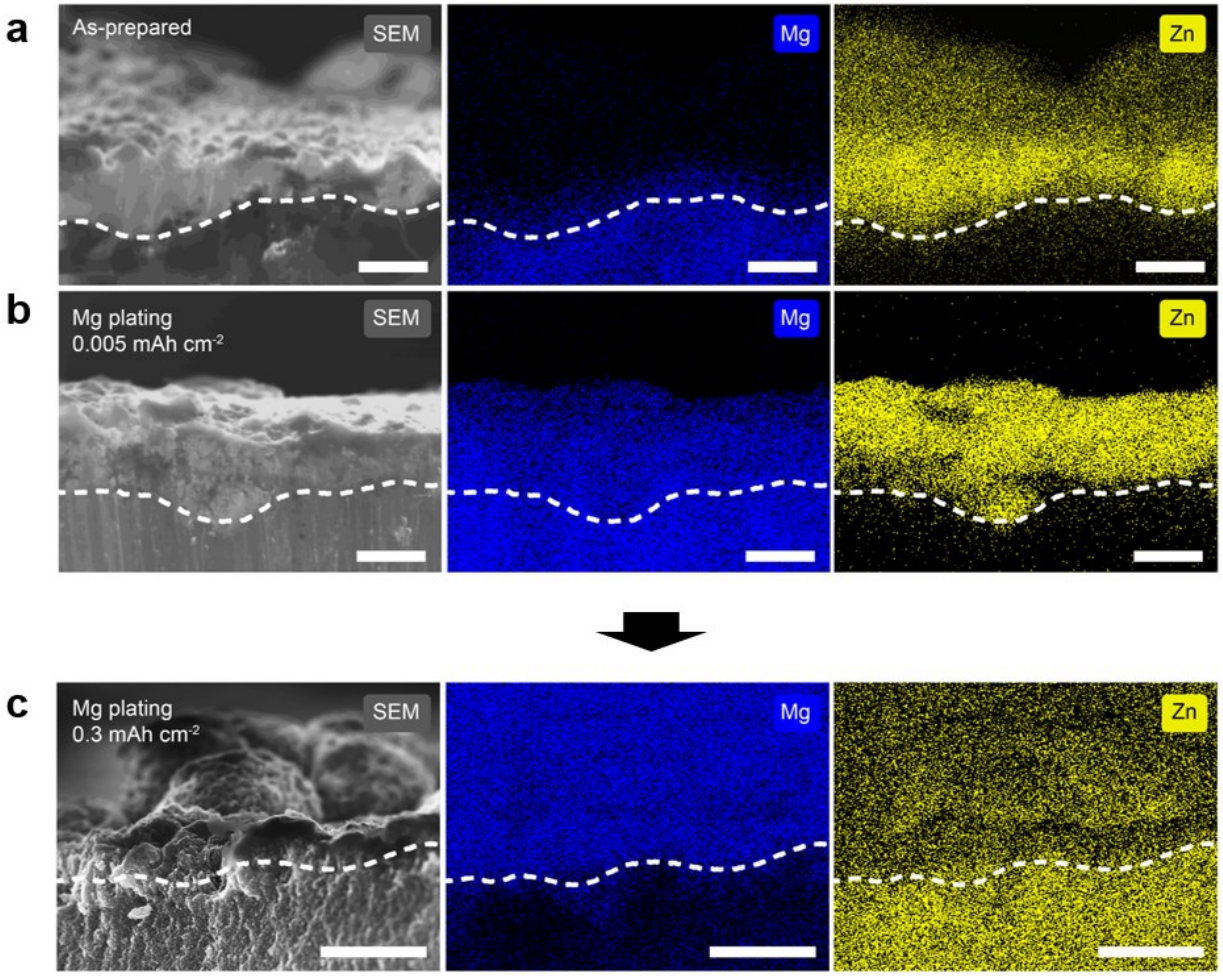

Figure S3. Cross-sectional SEM-EDX images during magnesiation for a) an as-prepared Zn-skeleton, b) a short-time plated Zn-skeleton (0.005 mAh cm^{-2}) and c) a long-time plated Zn-skeleton (0.3 mAh cm^{-2}). Scale bar = 5 μm.

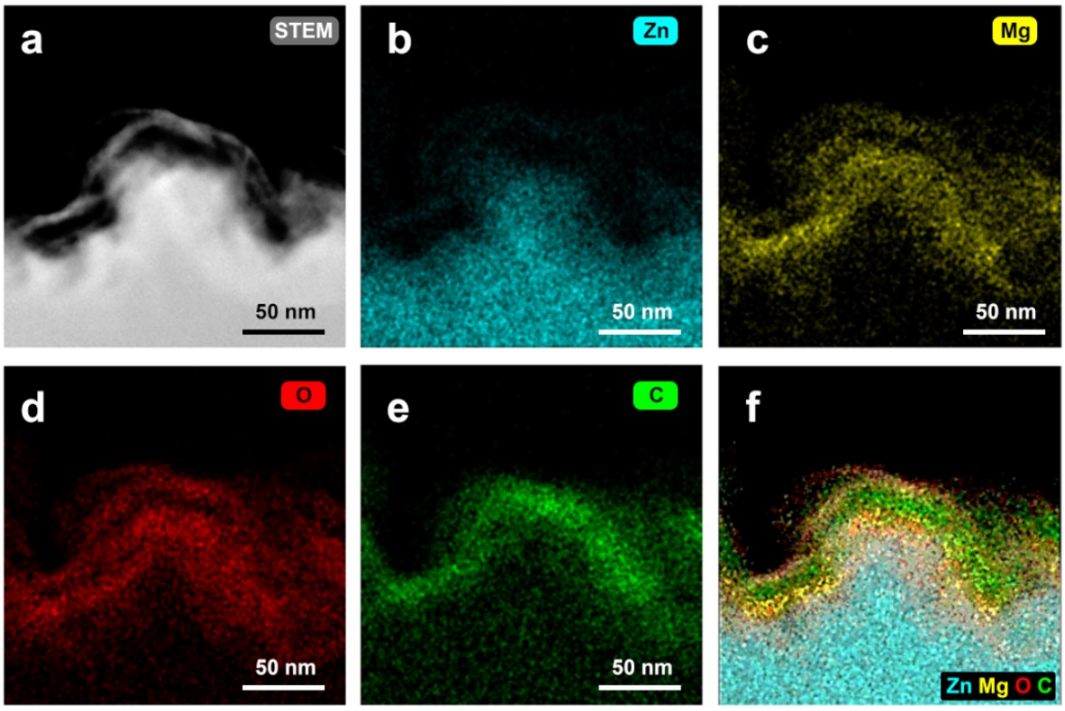

Figure S4. a) STEM image and corresponding elemental mapping for b) Zn, c) Mg, d) O, e) C, and f) overlapped mapping of Zn-skeleton after magnesiation.

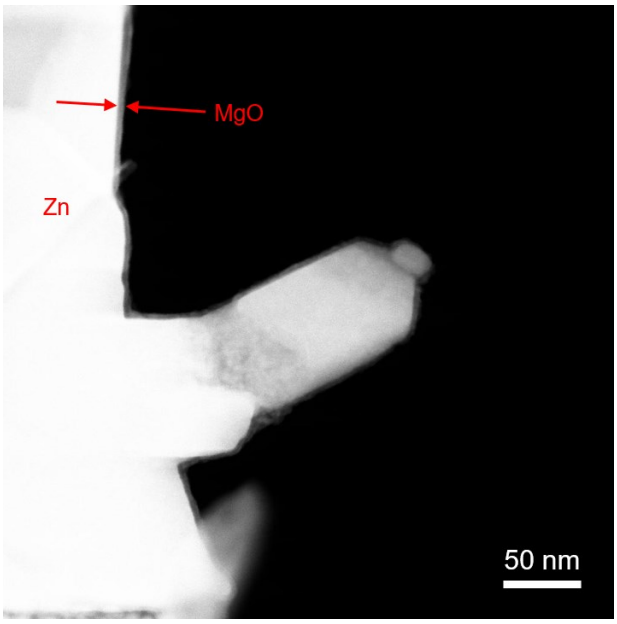

Figure S5. HR-STEM images of as-prepared Zn-skeleton where Zn-metal is covered by a thin layer of amorphous MgO.

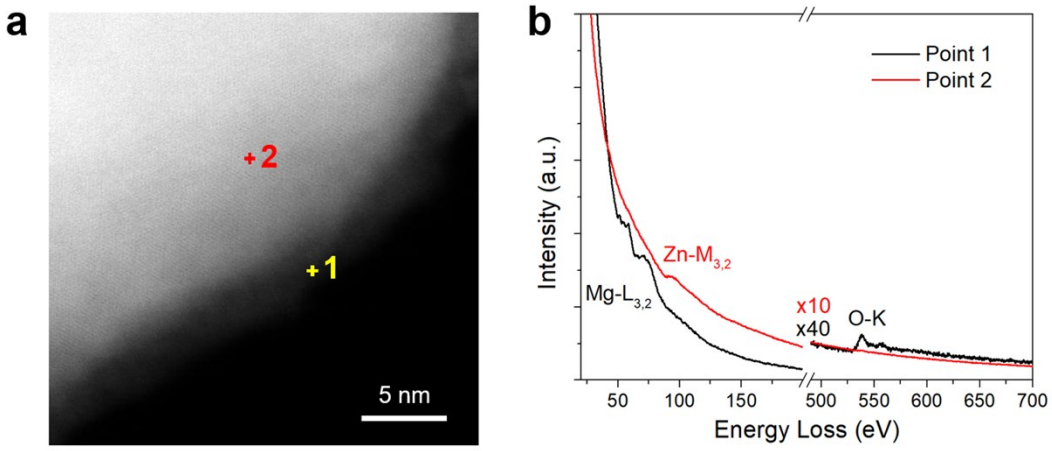

Figure S6. a) HR-STEM image and b) EELS spectra of as-prepared Zn-skeleton. The EELS was taken on amorphous MgO area (Point 1) and Zn-metal area (Point 2).

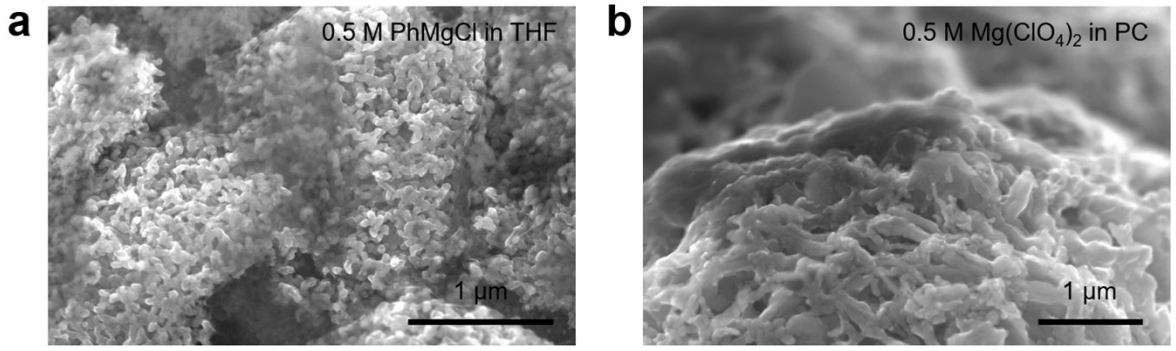

Figure S7. SEM images of the Mg nanoparticles deposited on Zn-skeleton in (a) 0.5 M PhMgCl in THF and (b) 0.5 M $Mg(ClO_4)_2$ in PC as electrolyte.

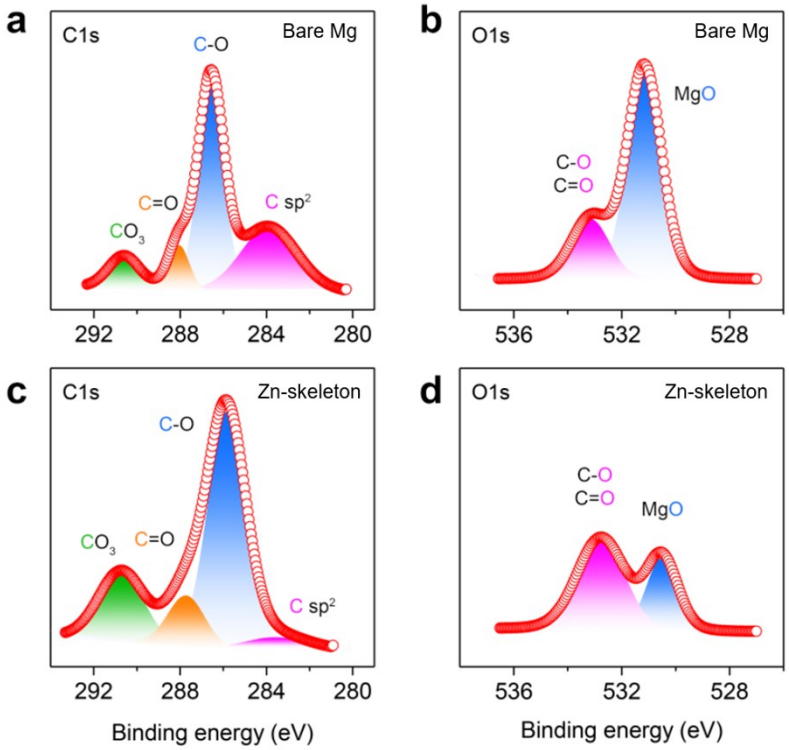

Figure S8. XPS spectra of a) C1s and b) O1s for the cycled bare Mg. XPS spectra of c) C1s and d) O1s for the cycled Zn-skeleton. XPS was conducted after Ar sputtering for 2 min. Both cells are cycled in 0.5 M $MgTFSI_2$ in PC.

It has been reported that the surface of Mg metal may demonstrate different O1s peaks, including $Mg(OH)_2$ (~530.5 eV) and MgO (~529.5 eV) [R1]. In other literature, the shift of binding energy of O1s may also come from MgO2 (~531 eV) and MgO (~530 eV) [R2]. Based on the XPS spectra, we speculate that bare Mg metal may have more impurities and decomposed products such as $Mg(OH)_2$ than Zn-skeleton.

From the C1s spectra, it can also be inferred that the decomposed solvent may participate in forming passivating components on bare Mg that may lead to a mixed peak of $Mg(OH)_2/MgCO_3$ and MgO with higher binding energy. The pre-existed amorphous MgO layer may prevent the decomposition of solvents but forming an Mg-MgO complex with a clear MgO peak (~529 eV).

However, it should be noted that the contamination from the atmosphere of the glove box and the solvent during the sample preparation may affect the surface film of Mg metal.

[R1]: "XPS Investigation of Surface Chemistry of Magnesium Electrodes in Contact with Organic Solutions of Organochloroaluminate Complex Salts" Langmuir 2003, 19, 2344-2348.

[R2]: "Conductive and Stable Magnesium Oxide Electron-Selective Contacts for Efficient Silicon Solar Cells" Adv. Energy Mater. 2017, 7, 1601863.

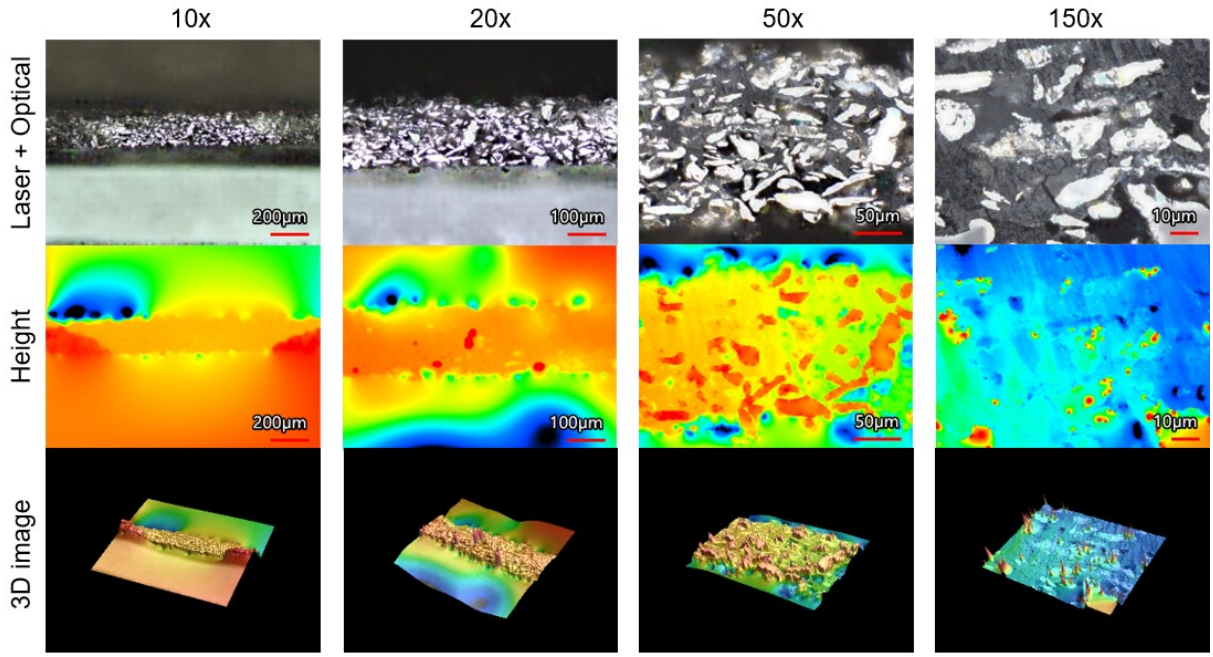

Figure S9. Laser-optical microscopic cross-sectional images of the Zn-skeleton coated Mg powder electrode. The sample has been prepared by cutting the cross-section by ion-milling.

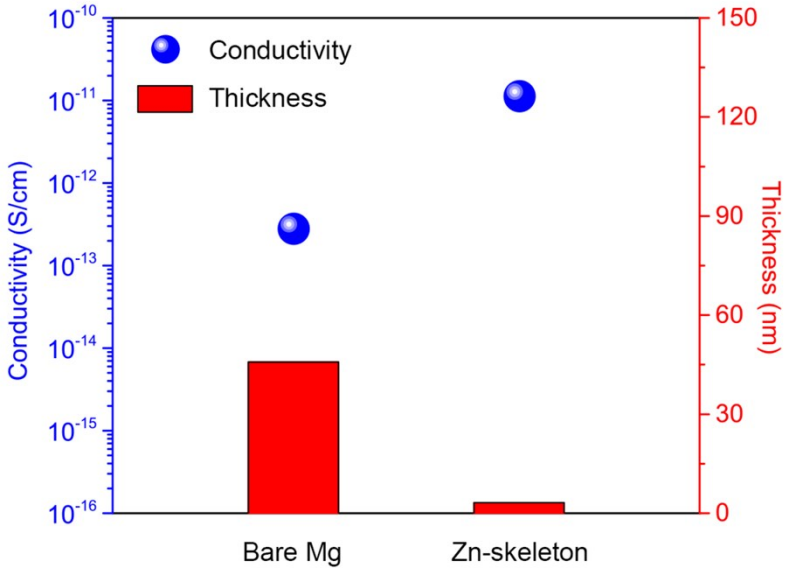

Figure S10. Interphase conductivities and thicknesses on bare Mg and Zn-skeleton. 0.5 M $Mg(ClO_4)_2$ in PC was used as an electrolyte.

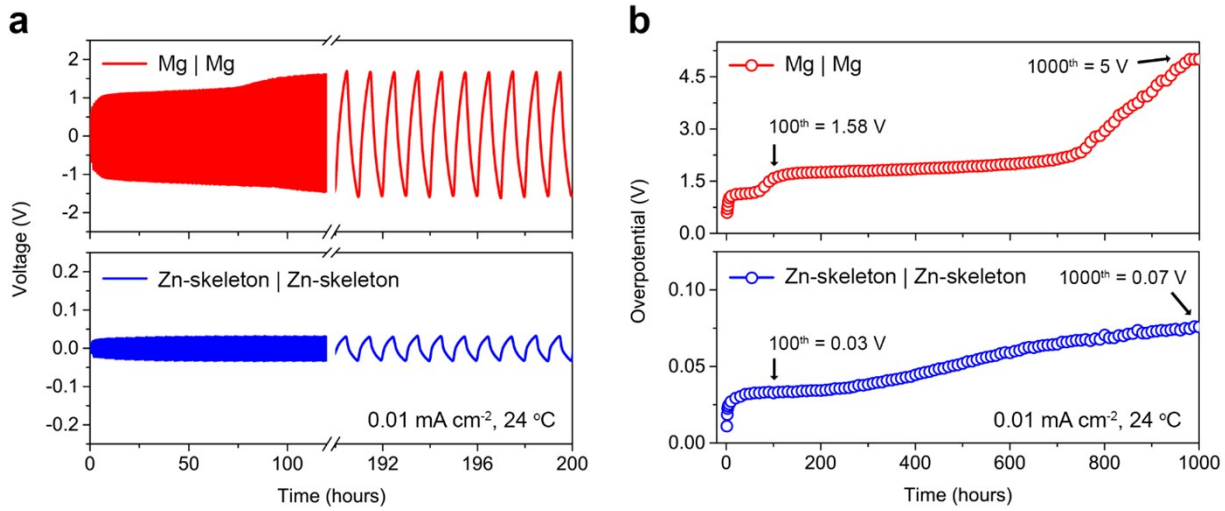

Figure S11. a) Plating/stripping voltage profiles and b) overpotentials of the symmetric bare Mg and Zn-skeleton cells. 0.5 M $Mg(ClO_4)_2$ in PC was used as an electrolyte. The Zn-skeleton has been previously magnesiated for 10 hrs before the symmetric cycling test.

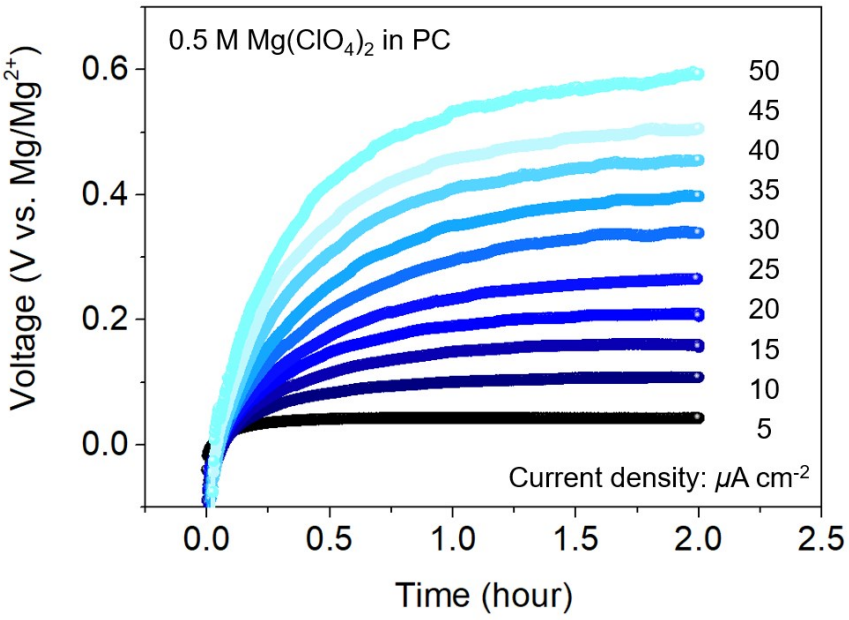

Figure S12. Voltage profile of the symmetric Zn-skeleton cell with increasing current densities from 5 to 50 μA cm^{-2} for 2 hours each step. 0.5 M $Mg(ClO_4)_2$ in PC was used as an electrolyte. A Zn-skeleton has been previously magnesiated for 0.15 mAh cm^{-2} before the symmetric cycling test.

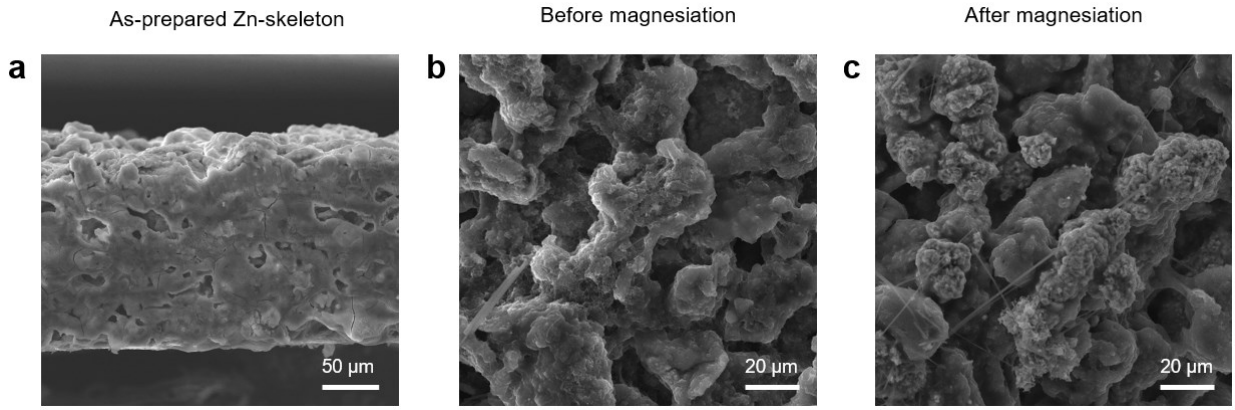

Figure S13. SEM images of a) cross-sectional and b,c) top surfaces of Zn-skeleton coated Mg powder electrode b) before and c) after magnesiation.

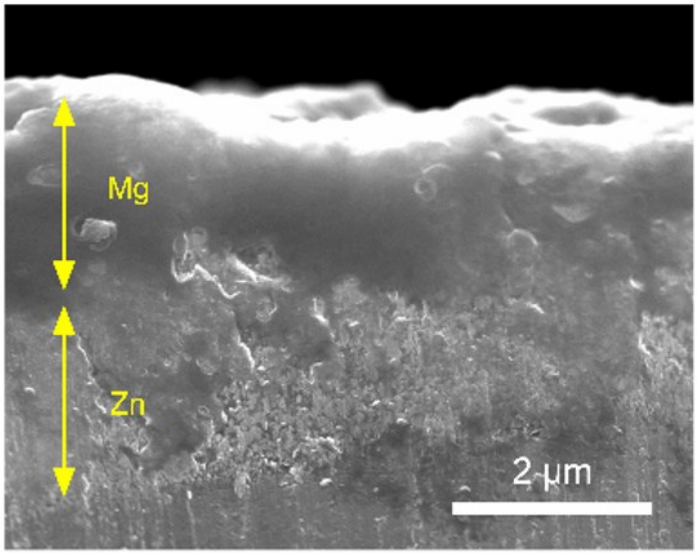

Figure S14. SEM image of asymmetric cell test with Zn foil. Zn-skeleton was magnesiated in 0.5 M PhMgCl in THF.

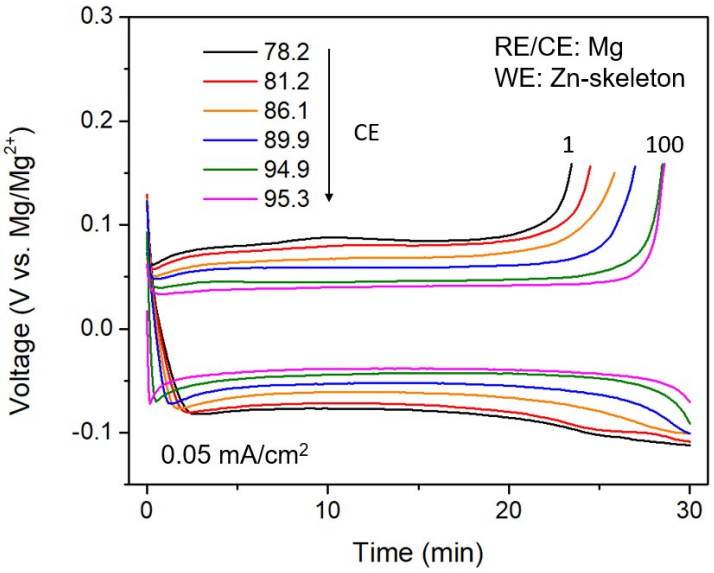

Figure S15. Coulombic efficiency of Mg plating/stripping on Zn-skeleton in 0.5 M PhMgCl in THF electrolyte. Mg powder electrode was used as reference/counter electrode while Zn-skeleton as working electrode. Zn-skeleton was magnesiated under 0.05 mA/cm^2 for 30 min, then demagnesiated with a cut-off voltage of 0.15 V. Coulombic efficiency (CE) is indicated in the plot with increasing cycle number (1st, 2nd, 5th, 10th, 50th, and 100th cycle).

It is difficult to measure the coulombic efficiency (CE) of Zn-skeleton in carbonate electrolytes due to the high resistance of the Mg metal reference electrode. Therefore, we tested our Zn-skeleton in 0.5 M PhMgCl in THF electrolyte. The CE increases as the cycle go by from 78.3% (1st cycle) to 95.3% (100th cycle), converging. It should be noted that the efficiency measured here will be different from that measured in carbonate electrolytes.

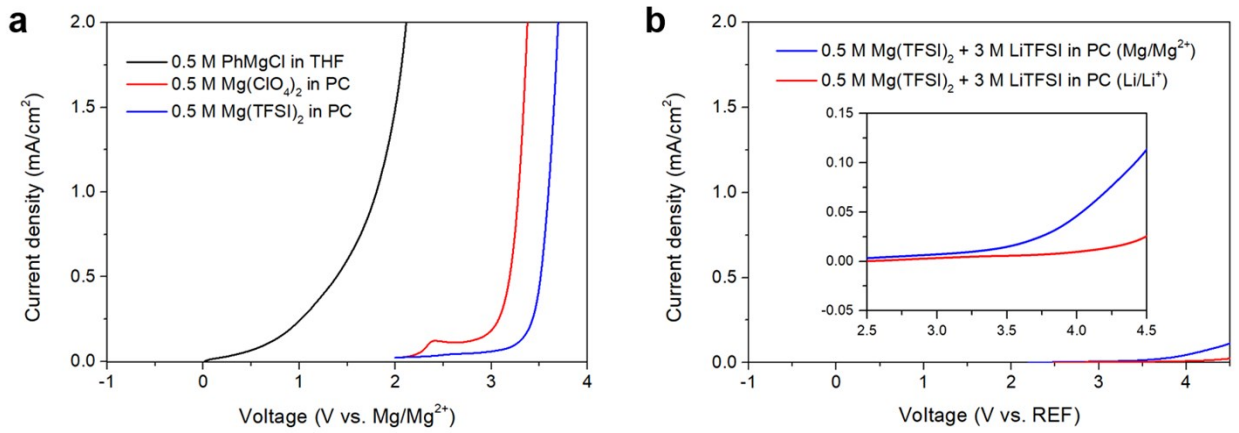

Figure S16. a) Linear sweep voltammetry of magnesium electrolytes: 0.5 M PhMgCl in THF (black), 0.5 M $Mg(ClO_4)_2$ in PC (red) and 0.5 M $Mg(TFSI)_2$ in PC (blue). The oxidative stability was investigated in a 3 electrode cell where magnesium ribbon was used as counter and reference electrode, while Pt (area = 0.0314 cm^2) was used as working electrode. b) Linear sweep voltammetry of hybrid electrolytes: 0.5 M $Mg(TFSI)_2$ + 3 M LiTFSI in PC. The scan rate was 20 mV/sec. For the hybrid electrolytes, either Mg or Li metal was used as reference/counter electrode in a coin cell while stainless-steel as working electrode.

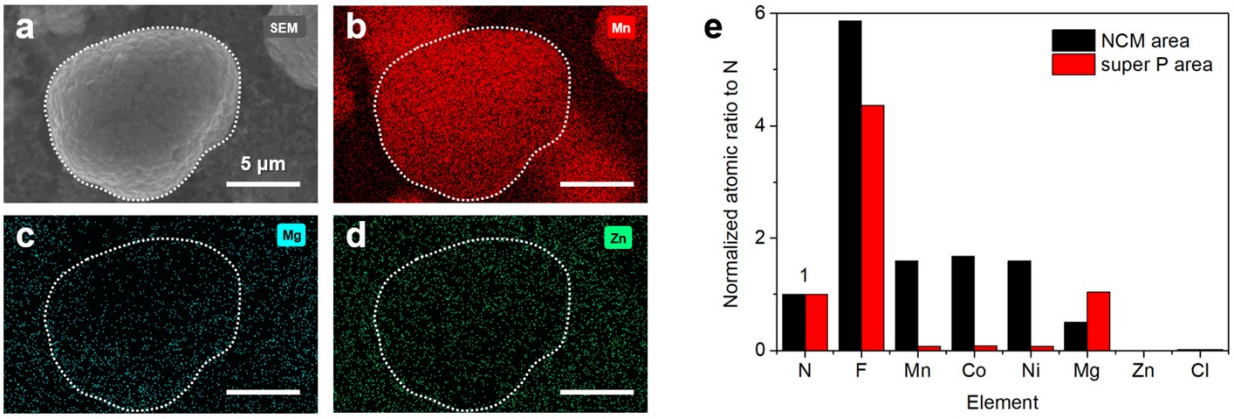

Figure S17. a) SEM image and corresponding elemental mapping of cycled NCM particles obtained from EDX with b) Mn, c) Mg, and d) Zn. e) Atomic ratio of the elements normalized to that of N.

EDX was taken on the NCM particle (black column) or on the area between particles (red column) where super P, PVDF and trance amount of electrolyte were assumed to be present. Almost no Zn and Cl were observed, indicating that Zn-skeleton on Mg current collector is stable and is not dissolved into the electrolyte.

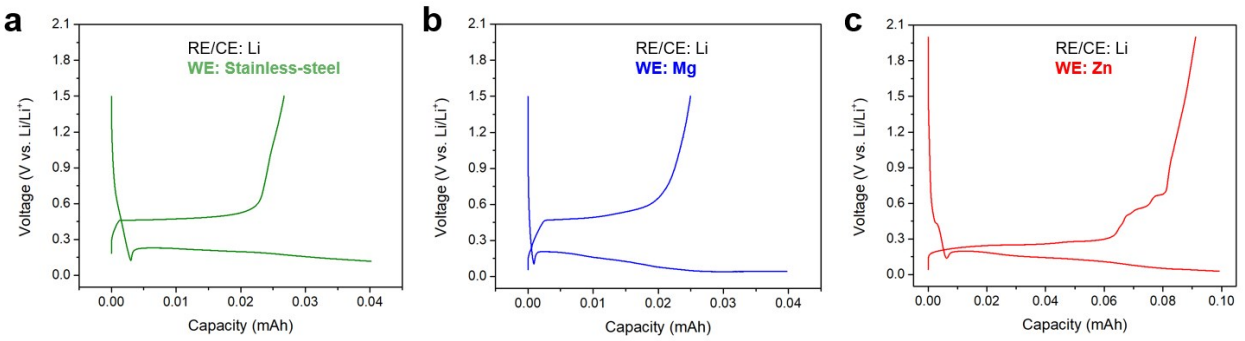

Figure S18. Voltage profiles of electrochemical cells where Li-metal was used as reference/counter electrode while a) stainless-steel, b) magnesium, and c) zinc were used as working electrode. A current density of 0.02 mA/cm^2 was applied. 3 M LiTFSI in PC was used as an electrolyte in a coin cell.

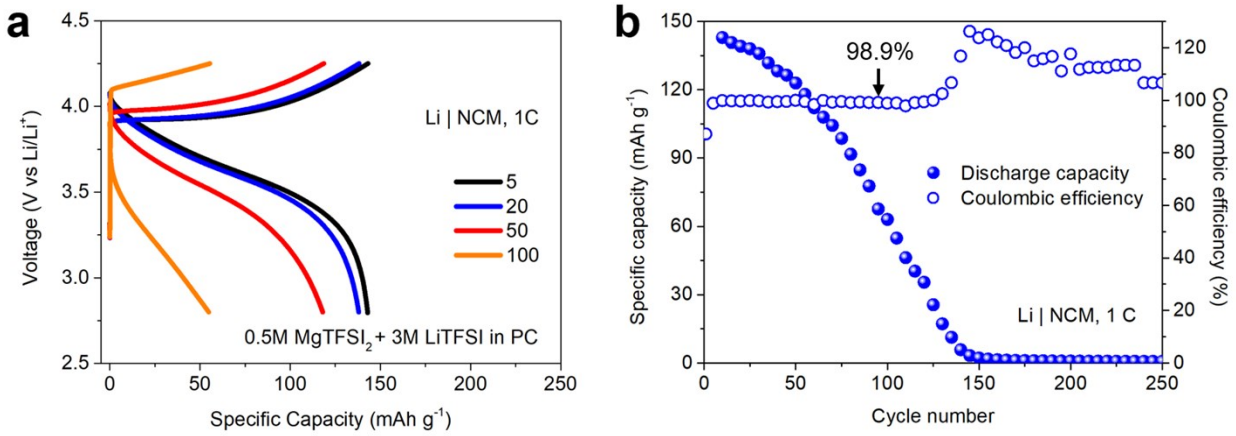

Figure S19. a) Voltage profiles and b) cycling performance of Li | NCM battery cycled at 1 C in 0.5 M $MgTFSI_2$ + 3 M LiTFSI in PC electrolyte.

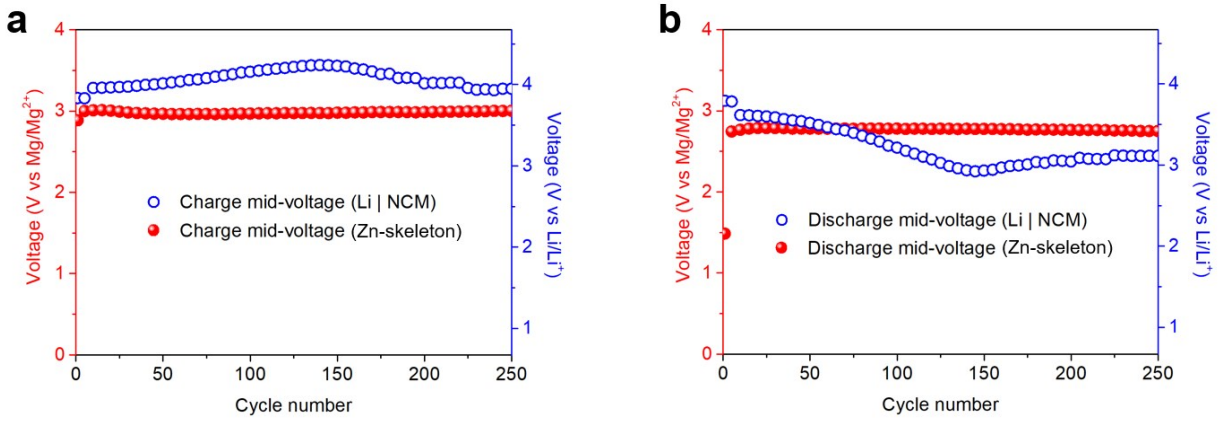

Figure S20. a) Charge-mid voltage and b) discharge-mid voltage of Li | NCM and Zn-skeleton | NCM batteries in 0.5 M $MgTFSI_2$ + 3 M LiTFSI in PC electrolyte.

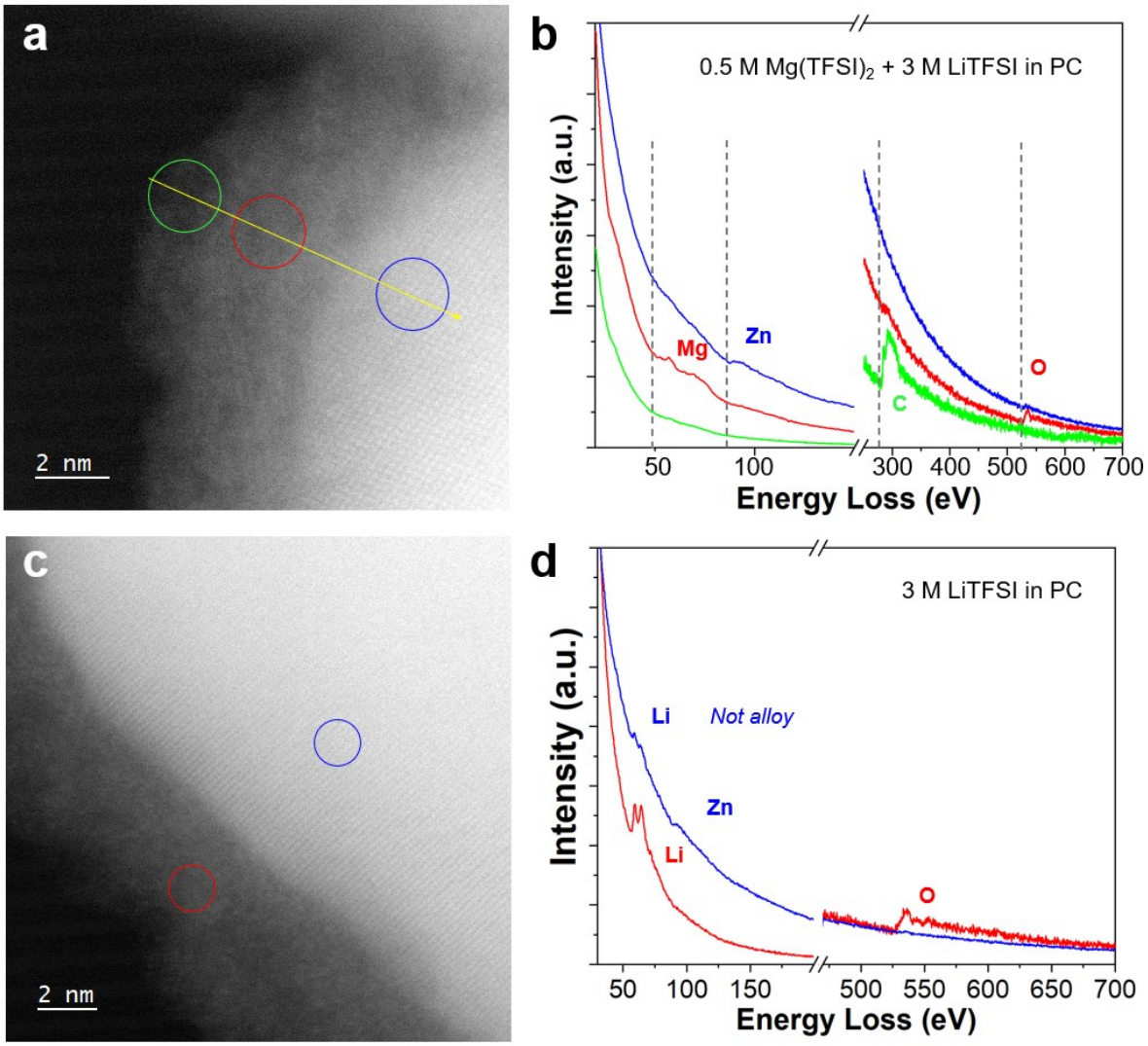

Figure S21. EELS study on the interphase of Zn-skeleton in a,b) 0.5 M $Mg(TFSI)_2$ + 3 M LiTFSI and c,d) 3 M LiTFSI in PC electrolytes. a,c) HR-STEM images and b,d) EELS spectra.

The EELS line profile acquired from the interphase of the Zn-skeleton cycled in the hybrid 0.5 M $Mg(TFSI)_2$ + 3 M LiTFSI in PC electrolyte shows the composition of carbonaceous/organic outer layer, Mg/MgO layer and Zn-skeleton. Note that almost no Li peak is detected in the MgO layer after cycled in the hybrid electrolyte, while great amount of oxidized Li peaks such as Li_2O, LiOH (~59, 64 eV) is recored when cycled in 3 M LiTFSI in PC electrolyte. This is possibly an evidence that the MgO layer prevents the deposition of Li at the surface of Zn skeleton. Interestingly, no Zn-Li or Mg-Li alloys have been detected as well. The Li peaks from the bulk Zn area (the blue spectrum in (d)) is from the oxidized Li covering the surface of Zn, but not composing alloy with Zn, as confirmed in the HR-STEM image with the pure Zn lattice.

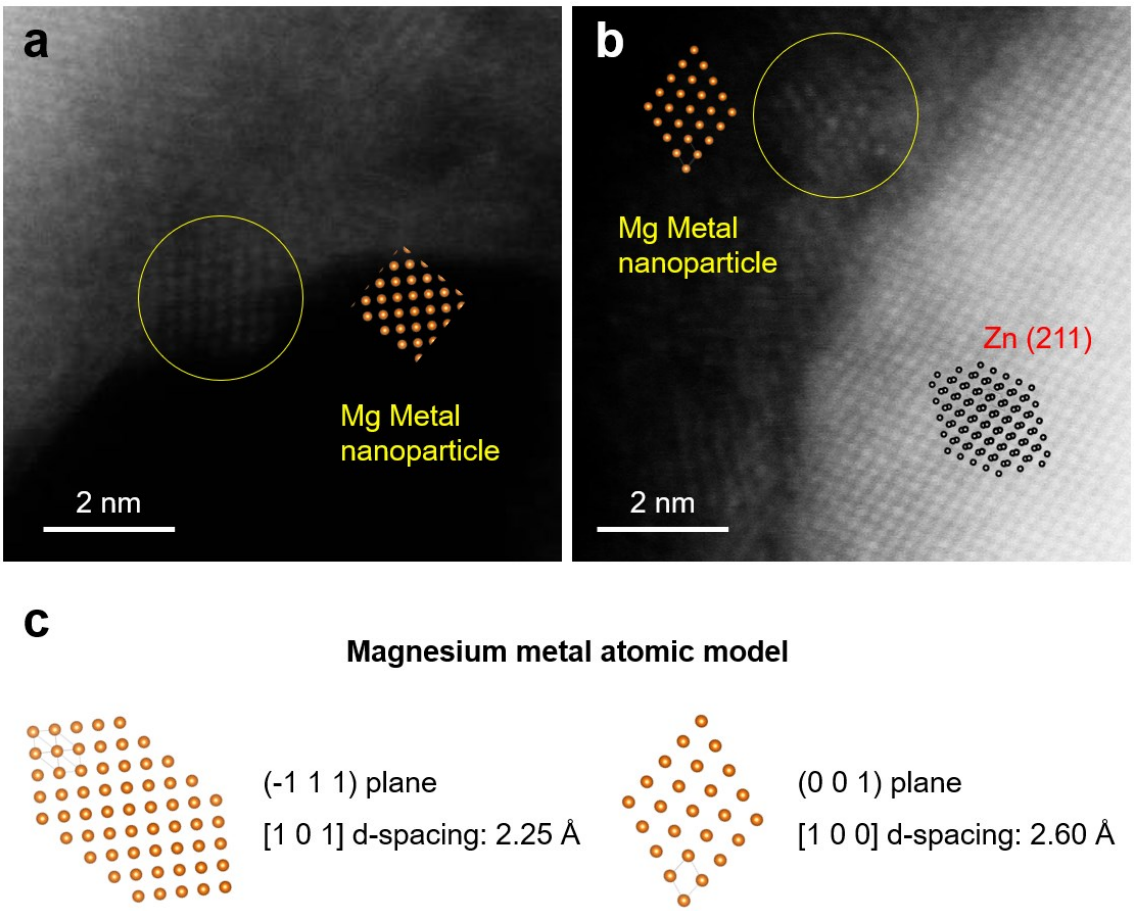

Figure S22. HR-STEM images of Mg metal nanocrystals in the amorphous/defective MgO layer on Zn-skeleton in the interphase near a) outer organic layer or b) Zn-skeleton. c) Magnesium metal atomic model in (-1 1 1) plane and (0 0 1) plane.